JYVÄSKYLÄN YLIOPISTO
UNIVERSITY OF JYVÄSKYLÄ

Neutron-proton pairing in the N=Z nuclei Mo-84

George Zimba

African School of Physics Seminar Series

Overview

Background


World Map
Kilometers
0 1000 2000 3000
0 1000 2000
Miles
Arctic Ocean
Atlantic Ocean
Pacific Ocean
Indian Ocean
Southern Ocean
Canada
United States
Mexico
Greenland (Denmark)
Iceland
Russia
Kazakhstan
Mongolia
China
Japan
India
Iran
Turkey
Saudi Arabia
Brazil
Peru
Bolivia
Chile
Argentina
Venezuela
Colombia
Ecuador
Algeria
Libya
Egypt
Mali
Niger
Chad
Sudan
South Sudan
Ethiopia
Nigeria
Democratic Republic of the Congo
Angola
Zambia
Namibia
Botswana
South Africa
Tanzania
Kenya
Madagascar
Indonesia
Philippines
Papua New Guinea
Australia
New Zealand
Hawaii (U.S.)
1. Burundi
2. Malawi
3. Rwanda
4. Armenia
5. Azerbaijan
6. Bahrain
7. Qatar
8. Albania
9. Andorra
10. Belgium
11. Bosnia and Herzegovina
12. Croatia
13. Czech Republic
14. Vatican City
15. Kosovo
16. Liechtenstein
17. Luxembourg
18. Moldova
19. Montenegro
20. North Macedonia
21. Netherlands
22. San Marino
23. Serbia
24. Slovenia
25. Switzerland
26. Saint Vincent and the Grenadines
2019 Copyright © Ontheworldmap.com
№A1904190010

Background

Introduction

The strong nuclear force is observed (and assumed) to be roughly equally strong between a proton-proton(pp) pair and a neutron-neutron(nn) pair (charge symmetry) and on average equally strong between a proton-neutron(pn) pair as between pp and nn pairs (charge independence).

- Charge symmetry;

$$V_{nn} = V_{pp}$$

- Charge independent;

$$V_{np} = (V_{nn} + V_{pp})/2$$

Charge symmetry and charge independence characteristics of the strong force gives rise to the concept of isospin symmetry.

Introduction

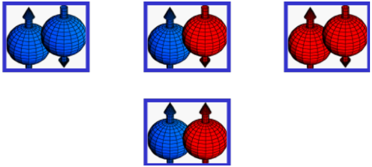

Protons and neutrons are distinguished by the z-component of isospin quantum number T:

- T$_{z,\pi}$ = -1/2 for protons (π)
- T$_{z,\nu}$ = +1/2 for neutrons (ν)

For multi-nucleon systems, the isospin projection (z-component) is defined as;

$$T_z = \frac{N - Z}{2}$$

Total isospin T for a nucleus with mass A,ranges from:

$$\frac{|N - Z|}{2} \quad \text{to} \quad \frac{A}{2}$$

And can not be less than its projection. Given T can have T_z numbers:

$$T_z = T, T - 1, ..., 0, ..., -T$$

Introduction

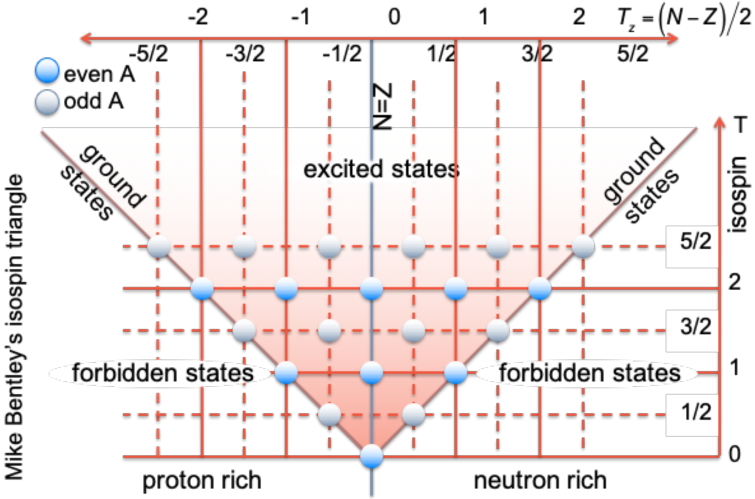

Figure 1: This figure shows the formation of isospin multiplets - different nuclei with different Tz have a set of states with the same isospin T (analog states). Without any isospin symmetry breaking forces the states would be degenerate in terms of excitation energy as indicated in this figure.

Introduction

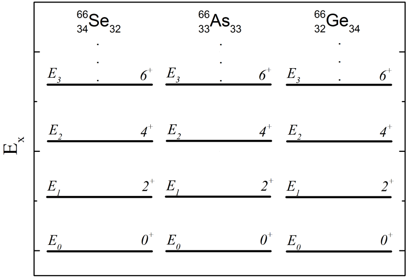

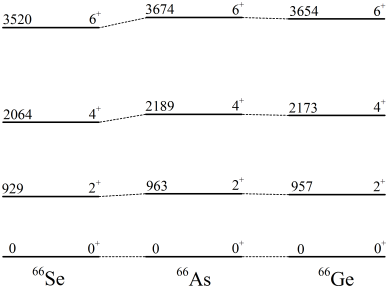

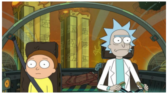

Introduction - np pairing

- For almost all known nuclei, i.e. those with N>Z ,the pair correlated state consists of neutron and/or proton pairs coupled to angular momentum J=0 and isospin T=1.
- Charge independence of the nuclear force implies that for N=Z nuclei, J=0, T=1 np pairing should exist on an equal footing with J=0, T=1 nn and pp pairing.
- However, it is still an open question whether strongly correlated J=1, T=0 np pairs also exist(deuteron-like pair condensate)

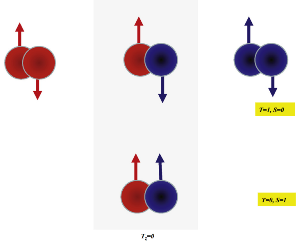

What would be the “fingerprint” of T=0, np pairing?

Introduction - np pairing

Theoretical and experimental efforts to find “fingerprints” of np pairing:

- Binding energies
- Low-lying states of odd-odd self-conjugate nuclei
- **Rotational response**
- Gamow-Teller β-decay
- Pairing vibrations
- ....

Theoretical Calculations

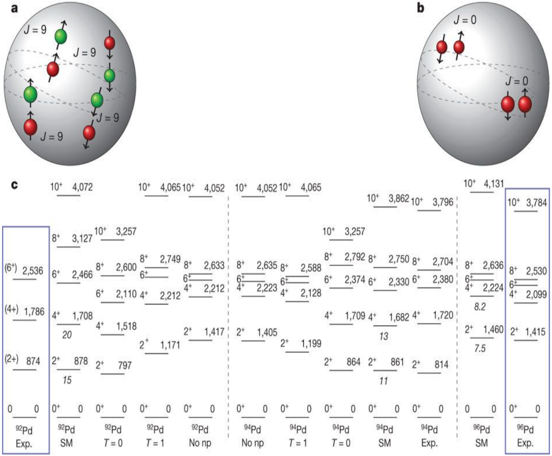

Figure 2: Schematic illustration of the structure of the ground-state wavefunction of ^{92}Pd in the spin-aligned np paired phase (green, neutron hole; red, proton hole). The experimental and calculated spectra for ^{92,94}Pd include, in addition to full Shell Model, also results for pure T=0 and pure T=1 np interactions [1]

- Evidence that the T=0 mode of the np interactions plays a role in $^{92}_{46}\mathrm{Pd}_{46}$?

Theoretical Calculations

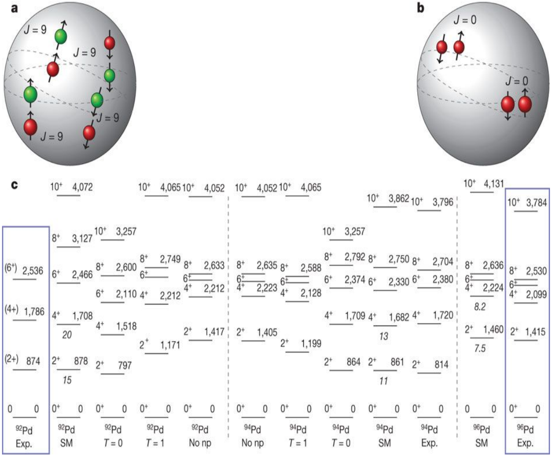

Figure 2: Schematic illustration of the structure of the ground-state wavefunction of ^{92}Pd in the spin-aligned np paired phase (green, neutron hole; red, proton hole). The experimental and calculated spectra for ^{92,94}Pd include, in addition to full Shell Model, also results for pure T=0 and pure T=1 np interactions [1]

- Evidence that the T=0 mode of the np interactions plays a role in $^{92}_{46}$Pd$_{46}$?
- This work provides some evidence for the presence of spin-aligned np pairing (T=0) phase. However further experimental information is needed to confirm this interpretation.

Theoretical Calculations

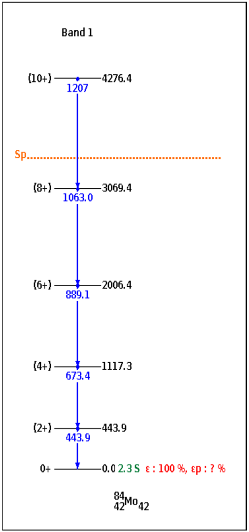

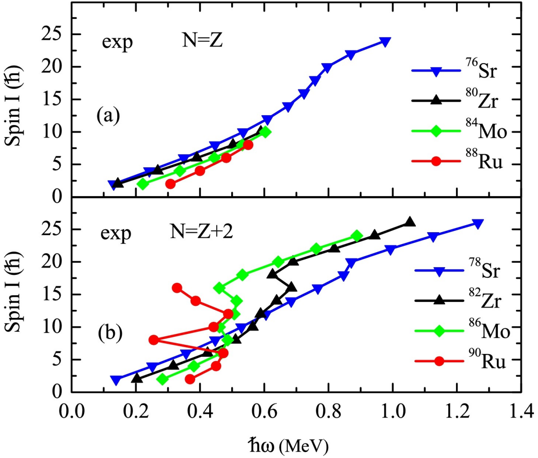

(b) Experimental $I - \omega$ plots for ground state bands of (a) N = Z ^{76}Sr, ^{80}Zr, ^{84}Mo, and ^{88}Ru, (b) N=Z+2 nuclei ^{78}Sr, ^{82}Zr, ^{86}M0, and ^{90}Ru [3] and reference herein

(a) Level scheme of ^{84}Mo [2]

Theoretical Calculations

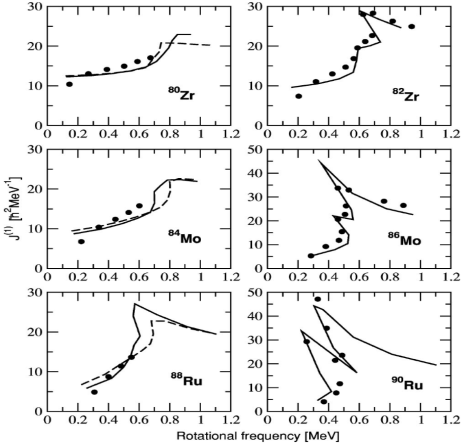

Figure 4: Comparison of experimental data(dots) and projected shell model calculations(PSM). The full lines are the PSM calculations with standard interaction, the dashed lines are PSM calculations with enhanced np residual interaction [2]

$$\hat{H} = \hat{H}_\nu + \hat{H}_\pi + \hat{H}_{\nu\pi}$$

Where $\hat{H}_{\pi\nu}$ is the np quadrupole-quadrupole residual interaction.

$$\hat{H} = -\chi_{\pi\nu} \sum_\mu \hat{Q}^{\dagger\mu}_\nu \hat{Q}^\mu_\pi$$

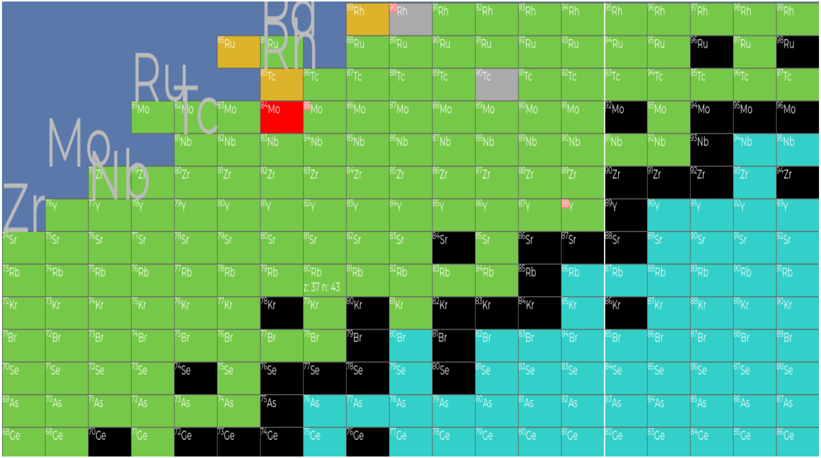

								^{89}Rh	^{90}Rh	^{91}Rh	^{92}Rh	^{93}Rh	^{94}Rh	^{95}Rh	^{96}Rh	^{97}Rh	^{98}Rh	^{99}Rh
					^{85}Ru	^{8}Ru		^{88}Ru	^{89}Ru	^{90}Ru	^{91}Ru	^{92}Ru	^{93}Ru	^{94}Ru	^{95}Ru	^{96}Ru	^{97}Ru	^{98}Ru
						^{85}Tc	^{86}Tc	^{87}Tc	^{88}Tc	^{89}Tc	^{90}Tc	^{91}Tc	^{92}Tc	^{93}Tc	^{94}Tc	^{95}Tc	^{96}Tc	^{97}Tc
			^{81}Mo	^{82}Mo	^{83}Mo	^{84}Mo	^{85}Mo	^{86}Mo	^{87}Mo	^{88}Mo	^{89}Mo	^{90}Mo	^{91}Mo	^{92}Mo	^{93}Mo	^{94}Mo	^{95}Mo	^{96}Mo
				^{81}Nb	^{82}Nb	^{83}Nb	^{84}Nb	^{85}Nb	^{86}Nb	^{87}Nb	^{88}Nb	^{89}Nb	^{90}Nb	^{91}Nb	^{92}Nb	^{93}Nb	^{94}Nb	^{95}Nb
		^{7}Zr	^{79}Zr	^{80}Zr	^{81}Zr	^{82}Zr	^{83}Zr	^{84}Zr	^{85}Zr	^{86}Zr	^{87}Zr	^{88}Zr	^{89}Zr	^{90}Zr	^{91}Zr	^{92}Zr	^{93}Zr	^{94}Zr
	^{76}Y	^{77}Y	^{78}Y	^{79}Y	^{80}Y	^{81}Y	^{82}Y	^{83}Y	^{84}Y	^{85}Y	^{86}Y	^{87}Y	^{88}Y	^{89}Y	^{90}Y	^{91}Y	^{92}Y	^{93}Y
^{74}Sr	^{75}Sr	^{76}Sr	^{77}Sr	^{78}Sr	^{79}Sr	^{80}Sr	^{81}Sr	^{82}Sr	^{83}Sr	^{84}Sr	^{85}Sr	^{86}Sr	^{87}Sr	^{88}Sr	^{89}Sr	^{90}Sr	^{91}Sr	^{92}Sr
^{73}Rb	^{74}Rb	^{75}Rb	^{76}Rb	^{77}Rb	^{78}Rb	^{79}Rb	^{80}Rb z: 37 n: 43	^{81}Rb	^{82}Rb	^{83}Rb	^{84}Rb	^{85}Rb	^{86}Rb	^{87}Rb	^{88}Rb	^{89}Rb	^{90}Rb	^{91}Rb
^{72}Kr	^{73}Kr	^{74}Kr	^{75}Kr	^{76}Kr	^{77}Kr	^{78}Kr	^{79}Kr	^{80}Kr	^{81}Kr	^{82}Kr	^{83}Kr	^{84}Kr	^{85}Kr	^{86}Kr	^{87}Kr	^{88}Kr	^{89}Kr	^{90}Kr
^{71}Br	^{72}Br	^{73}Br	^{74}Br	^{75}Br	^{76}Br	^{77}Br	^{78}Br	^{79}Br	^{80}Br	^{81}Br	^{82}Br	^{83}Br	^{84}Br	^{85}Br	^{86}Br	^{87}Br	^{88}Br	^{89}Br
^{70}Se	^{71}Se	^{72}Se	^{73}Se	^{74}Se	^{75}Se	^{76}Se	^{77}Se	^{78}Se	^{79}Se	^{80}Se	^{81}Se	^{82}Se	^{83}Se	^{84}Se	^{85}Se	^{86}Se	^{87}Se	^{88}Se
^{69}As	^{70}As	^{71}As	^{72}As	^{73}As	^{74}As	^{75}As	^{76}As	^{77}As	^{78}As	^{79}As	^{80}As	^{81}As	^{82}As	^{83}As	^{84}As	^{85}As	^{86}As	^{87}As
^{68}Ge	^{69}Ge	^{70}Ge	^{71}Ge	^{72}Ge	^{73}Ge	^{74}Ge	^{75}Ge	^{76}Ge	^{77}Ge	^{78}Ge	^{79}Ge	^{80}Ge	^{81}Ge	^{82}Ge	^{83}Ge	^{84}Ge	^{85}Ge	^{86}Ge

Figure 5: Table of nuclides [4]

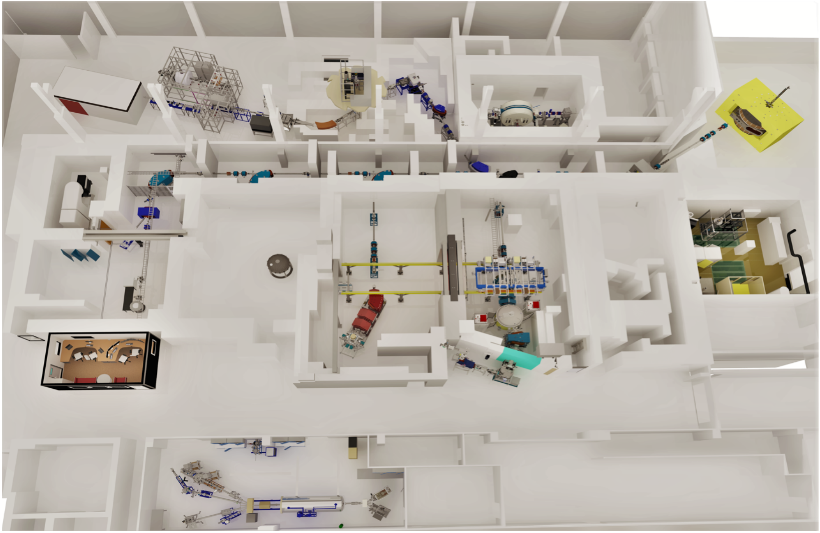

Experiment details

$$^{58}Ni +^{28} Si \longrightarrow^{86} Mo^{*} \longrightarrow^{84} Mo + 2n \text{ @ } E_{lab} = 201 MeV$$

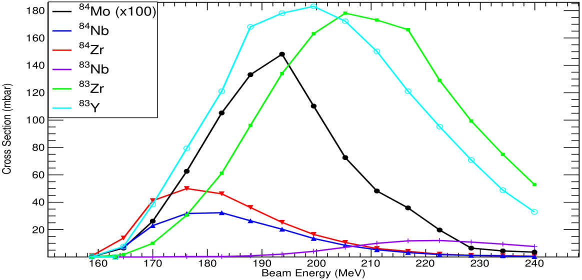

Figure 6: Theoretical cross section various evaporation channels for a ^{58}Ni beam and ^{28}Si target made using PACE4 code

Experiment details

Fusion recoils with specific mass are steered through the separator [5] and γ - rays detected using JUROGAM 3 [6](with 24 Compton-suppressed HpGe Clover detectors and 15 Phase 1 HpGe detectors).

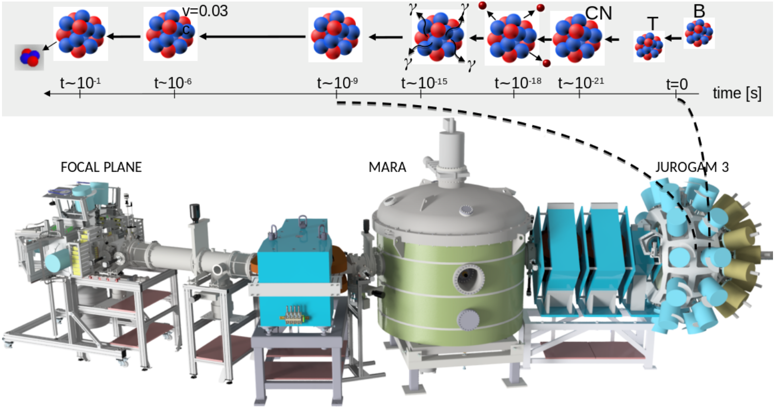

Experiment details

Fusion recoils with specific mass are steered through the separator [5] and γ - rays detected using JUROGAM 3 [6](with 24 Compton-suppressed HpGe Clover detectors and 15 Phase 1 HpGe detectors).

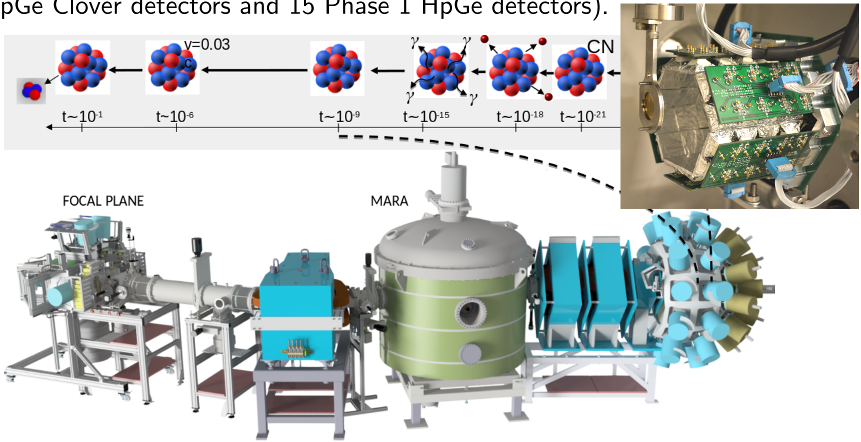

Experiment details

Fusion recoils with specific mass are steered through the separator [5] and γ - rays detected using JUROGAM 3 [6](with 24 Compton-suppressed HpGe Clover detectors and 15 Phase 1 HpGe detectors).

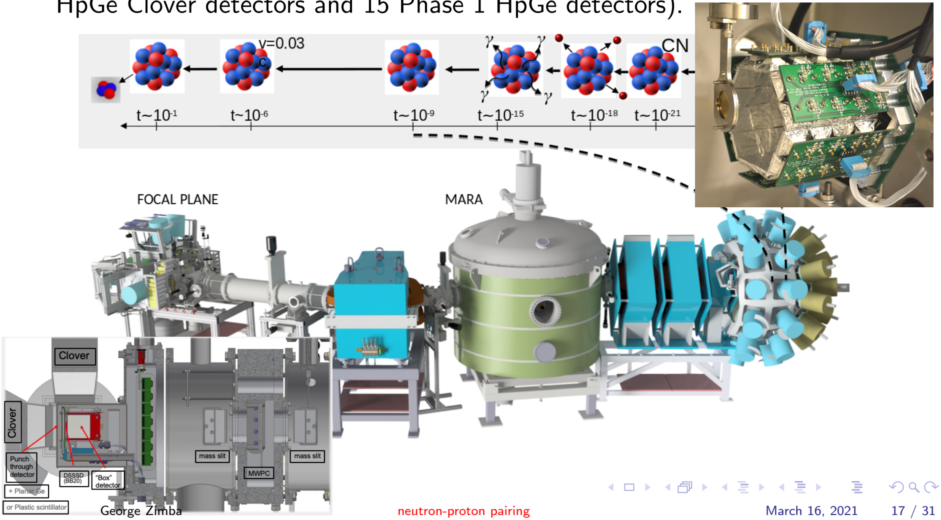

Experiment details

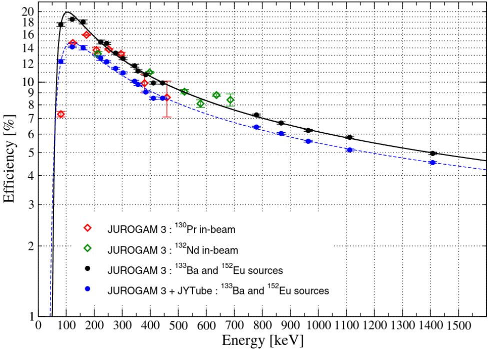

Figure 7: γ-ray detection efficiency of JUROGAM 3. Filled circles represent efficiencies determined with ^{133}Ba and ^{152}Eu calibration sources for the JUROGAM 3 array (black) and the JUROGAM 3 array combined with the JYTube detector (blue). Continuous and dashed lines are fit to the source data (corresponding colours). Open diamonds represent detection efficiency extracted from in-beam data obtained for ^{130}Pr (red) and ^{132}Nd (green) nuclei[6]

Table 1: Measured veto efficiency for Jyvaskyla charged particle veto tube detector(JYtube).

channel	Veto efficiency(%)
pn	83
2p	93
3p	96
4p	94

Results

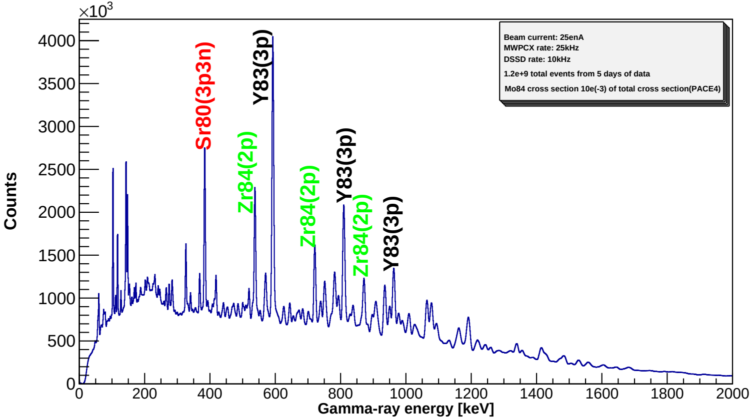

Figure 8: Raw juroGeE juroGeE X-projection. The ratio of the $2^+ \longrightarrow 0^+$ in ^{84}Zr to the total counts in the three nuclei(Zr, Sr and Y) are (a) 19%

Results

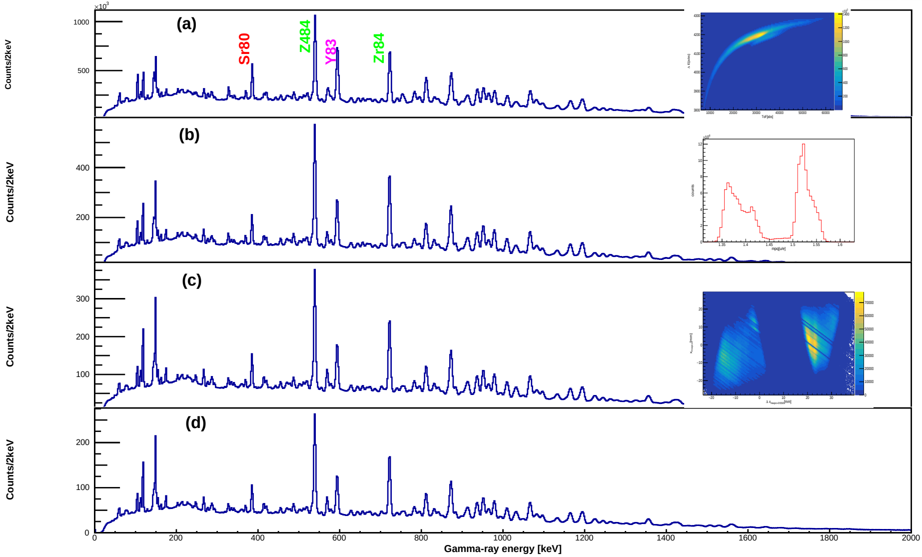

(a) Recoil juroGeE juroGeE projection X, (b) Recoil juroGeE juroGeE mpq projection X, (c) Recoil juroGeE juroGeE mwpcx projection X and (d) Recoil juroGeE juroGeE mpq mwpcx projection X. The ratio of the $2^{+} \longrightarrow 0^{+}$ in ^{84}Zr to the total counts in the three nuclei(Zr, Sr and Y) are (a) 47%, 60%, 64% and 60% respectively

Previous Results of ^{84}Mo

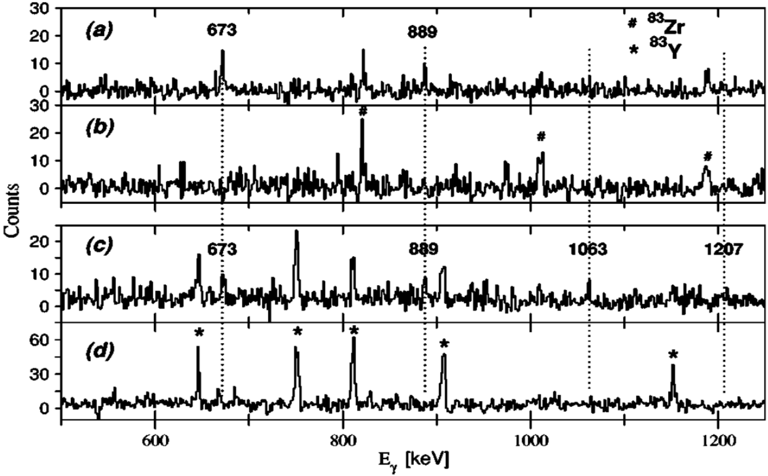

Figure 9: Gated γ-ray spectra showing the assignment of the yrast line in ^{84}Mo. The upper two spectra are gated by the 444keV transition,(a) $\gamma - \gamma$ matrix with veto on the charged particles and coincident with neutrons; (b)on $\gamma - \gamma$-matrix coincident with both neutrons and one proton. The lower two spectra are doubly gated spectra, with a gate 444keV/(673+889+1063 keV),(c) on $\gamma - \gamma - \gamma$ cube with veto on charged particles, and (d) on a $\gamma - \gamma - \gamma$ cube coincident with protons. The lines labeled with their energy have been assigned to the yrast band of ^{84}Mo.[2]

Current Results

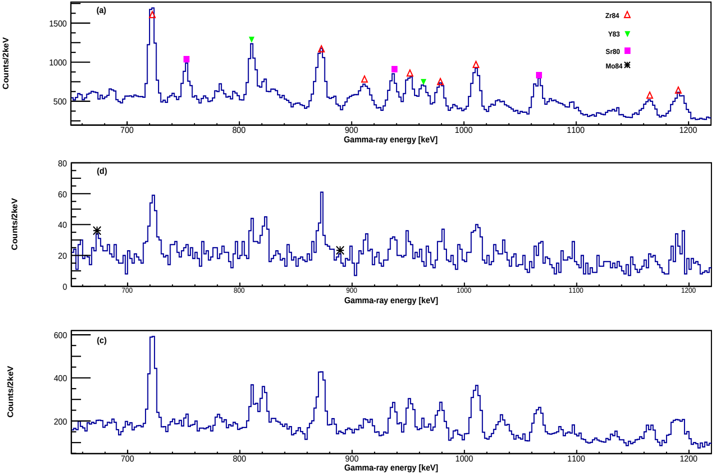

Figure 10: The spectra are gated by the 444keV transition,(a) recoil juroGeE $\gamma - \gamma$ matrix without any charged particle conditions; (b) on $\gamma - \gamma$-matrix coincident with veto on charged particle (c) n $\gamma - \gamma$-matrix coincident with one charged particle

Current Results

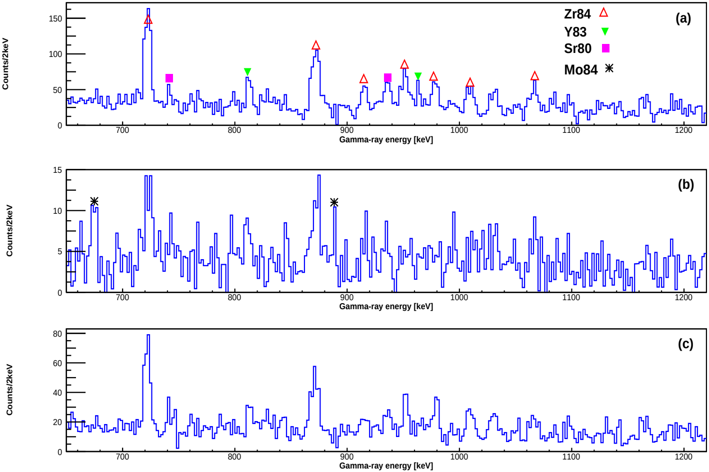

Figure 11: The spectra are gated by the 444keV transition,(a) on background subtracted recoil juroGeE $\gamma - \gamma$ matrix mass gated using mpq+mwpcx without any charged particle conditions; (b) on background subtracted $\gamma - \gamma$-matrix mass gated using mpq+mwpcx coincident with veto on charged particle (c) on background subtracted $\gamma - \gamma$-matrix mass gated using mpq+mwpcx coincident with one charged particle. The background is $\gamma - \gamma$-matrix outside juroGam time gate".

Current Results

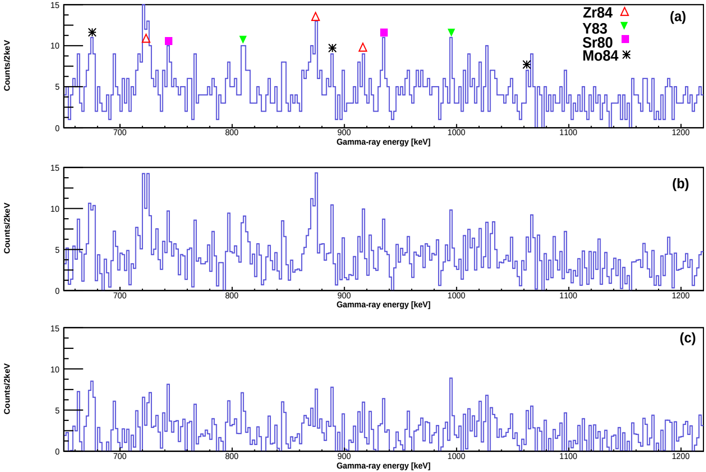

Figure 12: The spectra are gated by the 444keV transition,(a) recoil juroGeE $\gamma - \gamma$ matrix mass gated using mpq+mwpcx coincident with veto on charged particle; (b) on background subtracted $\gamma - \gamma$-matrix mass gated using mpq+mwpcx coincident with veto on charged particle; (c) on background subtracted $\gamma - \gamma$-matrix mass gated using mpq+mwpcx coincident with veto charged particle and charged particles subtracted. "The background is $\gamma - \gamma$-matrix outside juroGam time gate".

Current Results

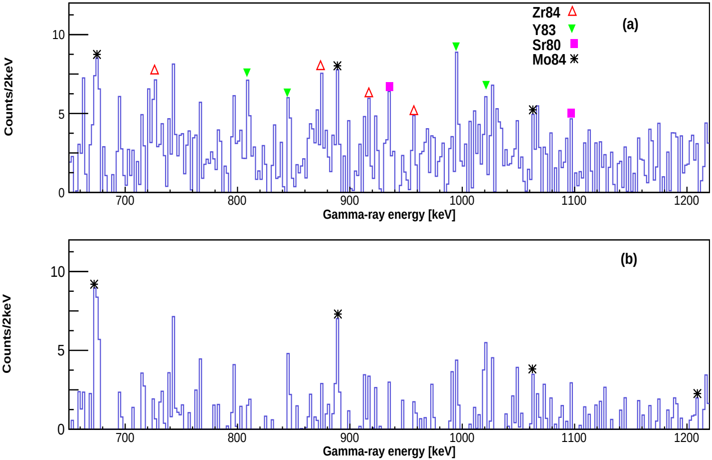

Figure 13: The spectra are gated by the 444keV transition,(a) on $\gamma - \gamma$-matrix mass gated using mpq+mwpcx coincident with veto charged particle and charged particles subtracted and (b) on $\gamma - \gamma$-matrix mass gated using mpq+mwpcx coincident with veto charged particle and charged particles subtracted without background

Current Results

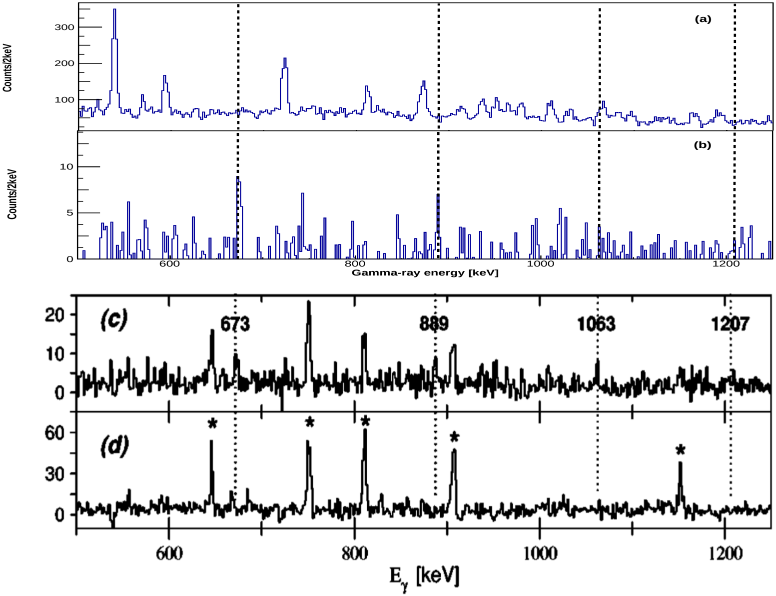

Conclusions

- Analysis is still in progress but it may be that new transitions above the currently proposed 10^+ state can not be discovered from this data.

Conclusions

- Analysis is still in progress but it may be that new transitions above the currently proposed 10^+ state can not be discovered from this data.
- In order to identify states above 10^+, we will require additional equipment such as ionization chamber.

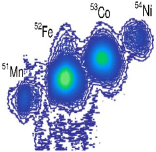

Typical particle identification after of a cocktail beam. Shown is the energy loss measured with the ionization chamber of the S800 focal plane vs. time of flight taken between two scintillators[7]

.

JYFL nuclear spectroscopy group

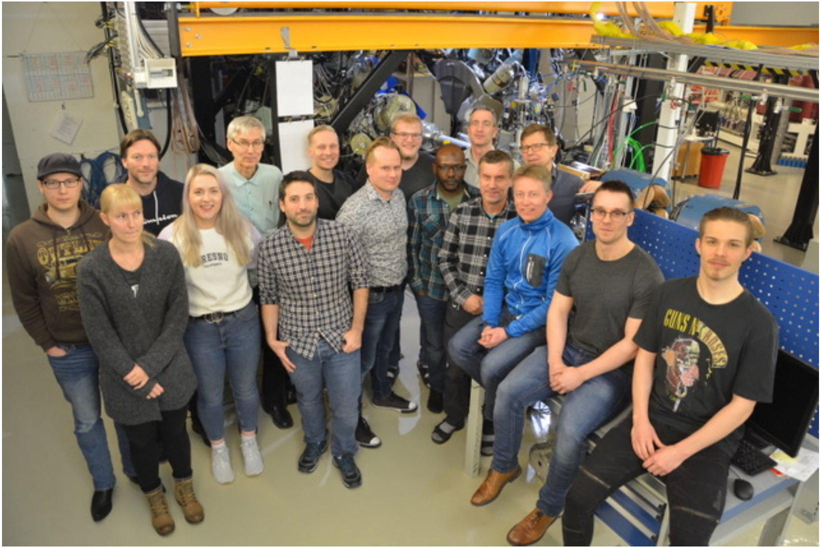

K. Auranen (KA) A. Briscoe(Missing), A. Illana Sison, R. Julin, H. Joukainen(Missing), H. Jutila, M. Leino, J. Louko, M. Luoma, J. Ojala, P. Rahkila, P. Ruotsalainen M. Sandzelius(Left) J. Sarén, H. Tann(Left), A. Tolosa Delgado(Missing), J. Uusitalo, and G. Zimba

Bibliography I

[1] B. Cederwall, F. Moradi, T. Bäck, and et al, “Evidence for a spin-aligned neutron–proton paired phase from the level structure of 92pd.,” *Nature*, vol. 469, pp. 68–71, 2011. [Online]. Available: https://doi.org/10.1038/nature09644.

[2] N. M ărginean, D. Bucurescu, C. Rossi Alvarez, C. A. Ur, Y. Sun, D. Bazzacco, S. Lunardi, G. de Angelis, M. Axiotis, E. Farnea, A. Gadea, M. Ionescu-Bujor, A. Iord ăchescu, W. Krolas, T. Kröll, S. M. Lenzi, T. Martinez, R. Menegazzo, D. R. Napoli, P. Pavan, Z. Podolyak, M. De Poli, B. Quintana, and P. Spolaore, “Delayed alignments in the $n = z$ nuclei $84\mathrm{Mo}$ and $88\mathrm{Ru}$,” *Phys. Rev. C*, vol. 65, p. 051 303, 5 Apr. 2002. DOI: 10.1103/PhysRevC.65.051303. [Online]. Available: https://link.aps.org/doi/10.1103/PhysRevC.65.051303.

Bibliography II

[3] K. Kaneko, Y. Sun, and G. de Angelis, "Enhancement of high-spin collectivity in n=z nuclei by the isoscalar neutron–proton pairing," *Nuclear Physics A*, vol. 957, pp. 144–153, 2017, ISSN: 0375-9474. DOI: https://doi.org/10.1016/j.nuclphysa.2016.08.007. [Online]. Available: https://www.sciencedirect.com/science/article/pii/S0375947416302147.

[4] [Online]. Available: https://www-nds.iaea.org/relnsd/vcharthtml/VChartHTML.html.

[5] J. Uusitalo, J. Saren, J. Partanen, and J. Hilton, "The jurogam3 spectrometer," *Acta Physica Polonica B*, vol. 50, no. 319, 2019.

[6] J. Pakarinen, "The jurogam3 spectrometer," *Eur. Phys. J. A*, vol. 56, no. 149, 2020.

Bibliography III

[7] A. Gade, D. Bazin, B. A. Brown, C. M. Campbell, J. A. Church, D.-C. Dinca, J. Enders, T. Glasmacher, P. G. Hansen, M. Honma, T. Mizusaki, W. F. Mueller, H. Olliver, T. Otsuka, L. A. Riley, J. R. Terry, J. A. Tostevin, and K. L. Yurkewicz, "Nuclear spectroscopy with fast exotic beams," *Journal of Physics: Conference Series*, vol. 20, pp. 95–100, Jan. 2005. DOI: `10.1088/1742-6596/20/1/016`. [Online]. Available: `https://doi.org/10.1088/1742-6596/20/1/016`.